

## **ANALYSIS OF SCATTERING WITH MULTI-SLOTTED CYLINDER WITH THICKNESS: TM CASE**

**W.-S. Lee\***, H.-L. Lee, H.-S. Jang, H.-S. Tae, and J.-W. Yu

Department of Electrical Engineering, KAIST, 291 Daehak-ro, Yuseong-gu, Daejeon 305-701, Korea

**Abstract**—An exact series solution for radiation and scattering of the dielectric-loaded multi-slotted cylinder with thickness is formulated by using radial mode matching technique. The radiated and guided fields are represented in terms of an infinite series of radial modes. By applying the appropriate boundary conditions, the coefficients of radiated and guided fields are obtained. The behaviors of resonance features are characterized for variation in frequencies, source positions, slot thickness, and dielectric coating properties.

### **1. INTRODUCTION**

A shield is the layer of conducting material which partially or completely envelops an electric circuit. It therefore affects the amount of electromagnetic radiation penetrating into the electric circuit from the external environment as well as the electromagnetic energy escaping from the electric circuit to the external environment. A variety of materials are used for shielding with a wide range of electrical conductivity, permittivity, magnetic permeability, and thickness. Shields invariably contain openings (apertures) for accessing and cooling and a number of joints and seams through which electromagnetic radiation can penetrate. When the envelope is slotted, environmental electromagnetic fields can create an important field inside the envelope, which can affect the electrical performance of the enclosed devices or circuits. In this case, the knowledge of the field distribution and polarization can help designers to choose the best layout and orientation for the most sensitive devices.

The slotted circular cylinder is one of the most investigated geometries in the area of scattering and radiation (Fig. 1). The

---

*Received 18 April 2012, Accepted 9 May 2012, Scheduled 18 May 2012*

\* Corresponding author: Wang-Sang Lee (wsang@kaist.ac.kr).

circular slotted cylinder has become the subject of extensive study due to its engineering applications in devices such as aperture and leaky wave antennas, microstrip transmission lines, microstrip antennas, composite missiles, and engine tubes of jet aircraft. The  $E$ -polarization case has the received attention in the researches with various techniques such as an integral equation approach by Senior [1] and by an approximate analytical approach [2]. Hussein and Hamid [3] have discussed the problem of the scattering by a perfectly conducting circular cylinder, with an infinite axial slot. The solution was later extended to include the problems of a multi-slotted circular cylinder [4]. The theory of the characteristic modes of a slot/slots in a conducting cylinder and their use for penetration and scattering was given in [5, 6]. The slotted cylinder, which is coated with an absorbing material either from inside or from outside, has been analyzed using the dual series based Riemann-Hilbert problem (RHP) technique in [7, 8]. Circular cylindrical surfaces covered periodically with the metallic strips and patches are considered in [9] using dual-series technique and in [10] using mixed spectral domain method (SDM), conjugated gradient method (CGM) and fast Fourier transform (FFT).

Although the problem in determining the electromagnetic scattering from and penetration of conducting cylinders with axial slots has been investigated by many researchers with various techniques [11–29], the determination of the transmitted field through multi-slotted circular cylinder in a thick conducting shell covered with dielectrics has received little attention. A simplified model of the problem to be solved here is represented by Fig. 2 and Fig. 3, where an electric line current is placed inside or outside a thick conducting cylindrical shell having multiple slots filled with a dielectric. The source produces an electromagnetic wave with its electric field vector parallel to the axis of the shell.

In this paper, an exact series solution for transmission and shielding effects of an electric line current placed inside or outside the multi-slotted circular cylinder in a thick conducting shell is developed for the first time by using a radial mode matching technique.

## 2. FORMULATION OF ELECTRICAL LINE CURRENT PLACED INSIDE

Consider an electric line current source inside the shell ( $\rho_i, \phi_i$ ) illuminating dielectric-coated multi-slotted circular cylinder with  $N$ th slot, as shown in Fig. 2. Throughout the work,  $e^{j\omega t}$  time harmonic factor is suppressed. In region (I) ( $\rho < a, k_o$ ), the total electric field can be represented as the sum of electric field of a line current and



**Figure 1.** Geometry of a single slotted circular cylinder, multi-slotted circular cylinder and concentrically loaded slotted circular cylinder.

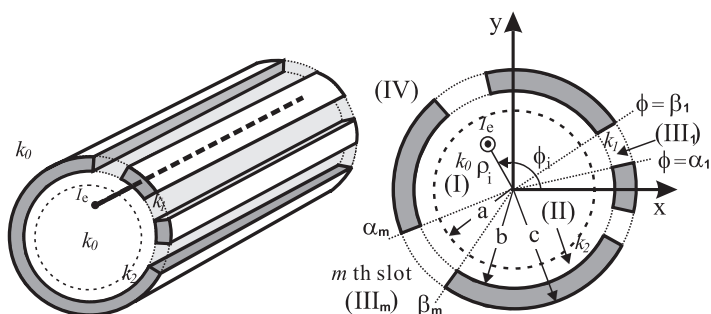


**Figure 2.** Geometry of an electrical line current placed inside a dielectric-loaded multi-slotted circular cylinder.

diffracted field, i.e.,

$$E_z^I(\rho, \phi) = E_o^I \begin{cases} \sum_{n=-\infty}^{\infty} \left\{ H_n^{(2)}(k_o \rho_i) J_n(k_o \rho) e^{-jn\phi_i} + D_n J_n(k_o \rho) \right\} e^{jn\phi}, & \rho < \rho_i \\ \sum_{n=-\infty}^{\infty} \left\{ J_n(k_o \rho_i) H_n^{(2)}(k_o \rho) e^{-jn\phi_i} + D_n J_n(k_o \rho) \right\} e^{jn\phi}, & \rho_i < \rho < a \end{cases} \quad (1)$$

where  $E_o^I = -\eta_o k_o I_e / 4$ ,  $\eta_o$  is the free space intrinsic impedance and  $I_e$  is the strength of the electric current filament,  $k_o$  is the free space wave number and  $J_n(\dots)$  and  $H_n^{(2)}(\dots)$  are Bessel function of the first kind and Hankel function of the second kind, respectively. In region (II) ( $a < \rho < b, k_2$ ), the electric field inside the dielectric coating can

be represented as

$$E_z^{II}(\rho, \phi) = E_o^l \sum_{n=-\infty}^{\infty} \left\{ J_n(k_o \rho) G_n(k_2 \rho) e^{-jn\phi} + D_n F_n(k_2 \rho) \right\} e^{jn\phi} \quad (2)$$

where

$$G_n(k_2 \rho) = \frac{1}{2} \pi k_2 a \left\{ H Y_n J_n(k_2 \rho) - H J_n Y_n(k_2 \rho) \right\}$$

$$F_n(k_2 \rho) = \frac{1}{2} \pi k_2 a \left\{ J Y_n J_n(k_2 \rho) - J J_n Y_n(k_2 \rho) \right\}$$

$$H Y_n(k_o a) = H_n^{(2)}(k_o a) Y_n'(k_2 a) - \frac{k_o}{k_2} H_n^{(2)'}(k_o a) Y_n(k_2 a)$$

$$H J_n(k_o a) = H_n^{(2)}(k_o a) J_n'(k_2 a) - \frac{k_o}{k_2} H_n^{(2)'}(k_o a) J_n(k_2 a)$$

$$J Y_n = J_n(k_o a) Y_n'(k_2 a) - \frac{k_o}{k_2} J_n'(k_o a) Y_n(k_2 a)$$

$$J J_n = J_n(k_o a) J_n'(k_2 a) - \frac{k_o}{k_2} J_n'(k_o a) J_n(k_2 a).$$

Here,  $k_o$  is the free space wave number and  $k_2 = k_o \sqrt{\epsilon_{r2}}$  while  $Y_n(\dots)$  is the Bessel function of the second kind. It is worth noting that the boundary conditions of the continuous tangential components of the electric and magnetic fields on the surface between the region (I) and region (II) are satisfied in Equation (2). The transmitted fields in the  $m$ th slot region (III<sub>m</sub>) ( $b < \rho < c$ ,  $\alpha_m < \phi < \beta_m$ ,  $k_1$ ) and region (IV) ( $\rho > c$ ,  $k_o$ ) can be expressed as follows

$$E_z^{III_m}(\rho, \phi) = E_o^l \sum_{p=1}^{\infty} \left\{ B_{p_m} J_{\mu_m}(k_1 \rho) + C_{p_m} Y_{\mu_m}(k_1 \rho) \right\} \sin \mu_m(\phi - \alpha_m) \quad (3)$$

$$E_z^{IV}(\rho, \phi) = E_o^l \sum_{n=-\infty}^{\infty} A_n H_n^{(2)}(k_o \rho) e^{jn\phi} \quad (4)$$

where  $\mu_m = p_m \pi / \phi_m$ ,  $\phi_m = \beta_m - \alpha_m$ ,  $p = 1, 2, 3, \dots$ ,  $m = 1, 2, \dots, N$  and  $k_1 = k_o \sqrt{\epsilon_{r1}}$ .

In order to determine the unknown coefficients  $A_n$ ,  $B_{p_m}$ ,  $C_{p_m}$  and  $D_n$ , the boundary conditions of the zero tangential electric field at the surface of conductor at  $\rho = b$  and  $c$  and continuous fields (i.e.,  $E_z$  and

$H_\phi$ ) across the aperture ( $\alpha_m < \phi < \beta_m, m = 1, 2, \dots, N$ ) are applied to obtain

$$B_{p_m} = -\frac{2}{\phi_m} \frac{Y'_{\mu_m}(k_1 b)}{\Delta_{\mu_m}} \frac{k_o}{k_1} \sum_{n=-\infty}^{\infty} A_n H_n^{(2)'}(k_o c) f_{n\mu}^m + \frac{2}{\phi_m} \frac{Y'_{\mu_m}(k_1 c)}{\Delta_{\mu_m}} \frac{k_2}{k_1} \sum_{n=-\infty}^{\infty} Z_n f_{n\mu}^m \quad (5)$$

$$C_{p_m} = \frac{2}{\phi_m} \frac{J'_{\mu_m}(k_1 b)}{\Delta_{\mu_m}} \frac{k_o}{k_1} \sum_{n=-\infty}^{\infty} A_n H_n^{(2)'}(k_o c) f_{n\mu}^m - \frac{2}{\phi_m} \frac{J'_{\mu_m}(k_1 c)}{\Delta_{\mu_m}} \frac{k_2}{k_1} \sum_{n=-\infty}^{\infty} Z_n f_{n\mu}^m \quad (6)$$

$$\sum_{n=-\infty}^{\infty} \sum_{m=1}^N A_n H_n^{(2)'}(k_o c) R_{kn}^m - \sum_{n=-\infty}^{\infty} \sum_{m=1}^N \left\{ \frac{F_n(k_2 b)}{F_n'(k_2 b)} \delta_{kn} - I_{kn}^m \right\} Z_n = J_k(k_o \rho_i) \left\{ G_k(k_2 b) - \frac{F_k(k_2 b)}{F_k'(k_2 b)} G_k'(k_2 b) \right\} e^{-jk\phi_i} \quad (7)$$

$$\sum_{n=-\infty}^{\infty} \sum_{m=1}^N \left\{ \delta_{kn} - \frac{H_n^{(2)'}(k_o c)}{H_n^{(2)}(k_o c)} Q_{kn}^m \right\} A_n H_n^{(2)'}(k_o c) = \sum_{n=-\infty}^{\infty} \sum_{m=1}^N Z_n M_{kn}^m \quad (8)$$

where  $\delta_{kn}$  is the Kronecker delta,

$$Z_n \equiv J_n(k_o \rho_i) G_n'(k_2 b) e^{-jn\phi_i} + D_n F_n'(k_2 b) \\ \Delta_{\mu_m} \equiv J'_{\mu_m}(k_1 b) Y'_{\mu_m}(k_1 c) - J'_{\mu_m}(k_1 c) Y'_{\mu_m}(k_1 b)$$

and

$$I_{kn}^m = \frac{1}{\pi \phi_m} \frac{k_2}{k_1} \sum_{p_m=1}^{\infty} \frac{J_{\mu_m}(k_1 b) Y'_{\mu_m}(k_1 c) - J'_{\mu_m}(k_1 c) Y_{\mu_m}(k_1 b)}{\Delta_{\mu_m}} f_{n\mu}^m \hat{f}_{k\mu}^m \\ R_{kn}^m = -\frac{2}{\pi^2 \phi_m} \frac{1}{k_1 b} \frac{k_o}{k_1} \sum_{p_m=1}^{\infty} \frac{f_{n\mu}^m \hat{f}_{k\mu}^m}{\Delta_{\mu_m}} \\ M_{kn}^m = \frac{2}{\pi^2 \phi_m} \frac{1}{k_1 c} \frac{k_2}{k_1} \sum_{p_m=1}^{\infty} \frac{f_{n\mu}^m \hat{f}_{k\mu}^m}{\Delta_{\mu_m}} \\ Q_{kn}^m = \frac{1}{\pi \phi_m} \frac{k_o}{k_1} \sum_{p_m=1}^{\infty} \frac{J'_{\mu_m}(k_1 b) Y_{\mu_m}(k_1 c) - J_{\mu_m}(k_1 c) Y'_{\mu_m}(k_1 b)}{\Delta_{\mu_m}} f_{n\mu}^m \hat{f}_{k\mu}^m$$

$$f_{n\mu}^m = \int_{\alpha_m}^{\beta_m} e^{jn\phi} \sin \mu_m(\phi - \alpha_m) d\phi$$

$$\hat{f}_{n\mu}^m = \int_{\alpha_m}^{\beta_m} e^{-jn\phi} \sin \mu_m(\phi - \alpha_m) d\phi.$$

Once the unknown coefficients  $A_n$  and  $D_n$  are determined from the simultaneous Equations (7) and (8),  $B_{p_m}$  and  $C_{p_m}$  can be evaluated by using the Equations (5) and (6).

### 3. FORMULATION OF ELECTRICAL LINE CURRENT PLACED OUTSIDE

Considering  $TM_z$  line source at  $(\rho_i, \phi_i)$  illuminating dielectric-loaded multi-slotted cylinder with  $N$ th slot, as shown in Fig. 3. The total electric field in regin (IV) ( $\rho > c, 0 < \phi < 2\pi, k_o$ ) can be represented by two parts: the incident and scattered fields as follows,

$$E_z^{IV}(\rho, \phi) = E_o^l \begin{cases} \sum_{n=-\infty}^{\infty} \left\{ s_n H_n^{(2)}(k_o \rho_i) J_n(k_o \rho) + A_n^o H_n^{(2)}(k_o \rho) \right\} e^{jn\phi}, & c < \rho < \rho_i \\ \sum_{n=-\infty}^{\infty} \left\{ s_n J_n(k_o \rho_i) H_n^{(2)}(k_o \rho) + A_n^o H_n^{(2)}(k_o \rho) \right\} e^{jn\phi}, & \rho > \rho_i \end{cases} \quad (9)$$

where  $E_o^l = -\eta_o k_o I_e / 4$ ,  $s_n = e^{-jn\phi_i}$ . In regions (I) ( $\rho < a, k_3$ ) and (II) ( $a < \rho < b, k_2$ ), the transmitted field inside the dielectric cylinder

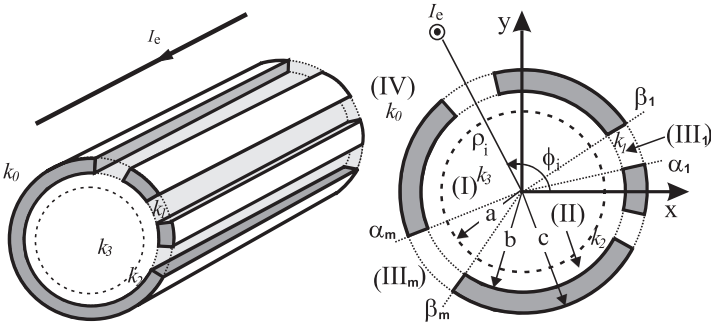


**Figure 3.** Geometry of an electrical line current placed outside the dielectric-loaded multi-slotted circular cylinder.

can be represented as

$$E_z^{II}(\rho, \phi) = E_o^l \sum_{n=-\infty}^{\infty} D_n^\circ F_n(k_2\rho)e^{jn\phi} \tag{10}$$

$$E_z^I(\rho, \phi) = E_o^l \sum_{n=-\infty}^{\infty} D_n^\circ J_n(k_3\rho)e^{jn\phi} \tag{11}$$

where

$$F_n(k_2\rho) = \frac{1}{2}\pi k_2 a \left\{ JY_n J_n(k_2\rho) - J J_n Y_n(k_2\rho) \right\}$$

$$JY_n = J_n(k_1 a) Y_n'(k_2 a) - \frac{k_1}{k_2} J_n'(k_1 a) Y_n(k_2 a)$$

$$J J_n = J_n(k_1 a) J_n'(k_2 a) - \frac{k_1}{k_2} J_n'(k_1 a) J_n(k_2 a)$$

Assuming that region (I) is filled with the conducting core, the above equation can be expressed as follows

$$E_z^{II}(\rho, \phi) = E_o^l \sum_{n=-\infty}^{\infty} D_n^\circ F_n(k_2\rho)e^{jn\phi}$$

$$E_z^I(\rho, \phi) = 0$$

where

$$F_n(k_2\rho) = \frac{1}{2}\pi k_2 a \left\{ J_n(k_2\rho) Y_n(k_2 a) - J_n(k_2 a) Y_n(k_2\rho) \right\}$$

In the  $m$ th slot region (III<sub>m</sub>) ( $\alpha_m \leq \phi \leq \beta_m, b < \rho < c, k_1$ ), the total fields  $E_z^{III_m}(\rho, \phi)$  can be represented as the summation of wedged-plate waveguide modes,

$$E_z^{III_m}(\rho, \phi) = E_o^l \sum_{p_m=1}^{\infty} \left\{ B_{p_m}^\circ J_{\mu_m}(k_1\rho) + C_{p_m}^\circ Y_{\mu_m}(k_1\rho) \right\} \sin \mu_m(\phi - \alpha_m) \tag{12}$$

To determine the unknown coefficients  $A_n^\circ, B_{p_m}^\circ, C_{p_m}^\circ$  and  $D_n^\circ$ , the boundary conditions of the zero tangential electric field at the surface of conductor at  $\rho = b$  and  $\rho = c$  and continuous fields across the aperture ( $\alpha_m < \phi < \beta_m, m = 1, 2, \dots, N$ ) are applied to obtain

$$B_{p_m}^\circ = \frac{2}{\phi_m} \frac{Y_{\mu_m}'(k_1 c)}{\Delta_{\mu_m}} \frac{k_2}{k_1} \sum_{n=-\infty}^{\infty} D_n^\circ F_n'(k_2 b) f_{n\mu}^m - \frac{2}{\phi_m} \frac{Y_{\mu_m}'(k_1 b)}{\Delta_{\mu_m}} \frac{k_o}{k_1}$$

$$\sum_{n=-\infty}^{\infty} \left\{ s_n H_n^{(2)}(k_o \rho_i) J_n'(k_o c) + A_n^\circ H_n^{(2)'}(k_o c) \right\} f_{n\mu}^m \tag{13}$$

$$C_{p_m}^\circ = -\frac{2}{\phi_m} \frac{J_{\mu_m}'(k_1 c) k_2}{\Delta_{\mu_m} k_1} \sum_{n=-\infty}^{\infty} D_n^\circ F_n'(k_2 b) f_{n\mu}^m + \frac{2}{\phi_m} \frac{J_{\mu_m}'(k_1 b) k_o}{\Delta_{\mu_m} k_1} \sum_{n=-\infty}^{\infty} \left\{ s_n H_n^{(2)}(k_o \rho_i) J_n'(k_o c) + A_n^\circ H_n^{(2)'}(k_o c) \right\} f_{n\mu}^m \quad (14)$$

$$s_k H_k^{(2)}(k_o \rho_i) J_k'(k_o c) + A_k^\circ H_k^{(2)'}(k_o c) = \sum_{m=1}^N \sum_{n=-\infty}^{\infty} D_n^\circ F_n'(k_2 b) M_{nk}^m + \sum_{m=1}^N \sum_{n=-\infty}^{\infty} \left\{ s_n H_n^{(2)}(k_o \rho_i) J_n'(k_o c) + A_n^\circ H_n^{(2)'}(k_o c) \right\} Q_{nk}^m \quad (15)$$

$$D_k^\circ F_k(k_2 b) = \sum_{m=1}^N \sum_{n=-\infty}^{\infty} D_n^\circ F_n'(k_2 b) I_{nk}^m + \sum_{m=1}^N \sum_{n=-\infty}^{\infty} \left\{ s_n H_n^{(2)}(k_o \rho_i) J_n'(k_o c) + A_n^\circ H_n^{(2)'}(k_o c) \right\} R_{nk}^m \quad (16)$$

The above simultaneous equation can be rewritten in the following matrix form

$$\begin{pmatrix} \Psi_1 & \Psi_2 \\ \Psi_3 & \Psi_4 \end{pmatrix} \begin{pmatrix} s_n H_n^{(2)}(k_o \rho_i) J_n'(k_o c) + A_n^\circ H_n^{(2)'}(k_o c) \\ D_n^\circ F_n(k_2 b) \end{pmatrix} = \begin{pmatrix} \Gamma \\ 0 \end{pmatrix} \quad (17)$$

where  $A_n$  and  $D_n$  are column vectors and  $\Psi_1, \Psi_2, \Psi_3, \Psi_4$ , and  $\Gamma$  are matrices whose elements are

$$\begin{aligned} \psi_{1,nk} &= \sum_{m=1}^N Q_{nk}^m - \frac{H_n^{(2)}(k_o c)}{H_n^{(2)'}(k_o c)} \delta_{nk} \\ \psi_{2,nk} &= \sum_{m=1}^N \frac{F_n'(k_2 b)}{F_n(k_2 b)} M_{nk}^m \\ \psi_{3,nk} &= -\sum_{m=1}^N R_{nk}^m \\ \psi_{4,nk} &= \delta_{nk} - \sum_{m=1}^N \frac{F_n'(k_2 b)}{F_n(k_2 b)} I_{nk}^m \\ \gamma_n &= -\frac{2j}{\pi k_o c} \frac{s_n H_n^{(2)}(k_o c)}{H_n^{(2)'}(k_o c)}. \end{aligned}$$

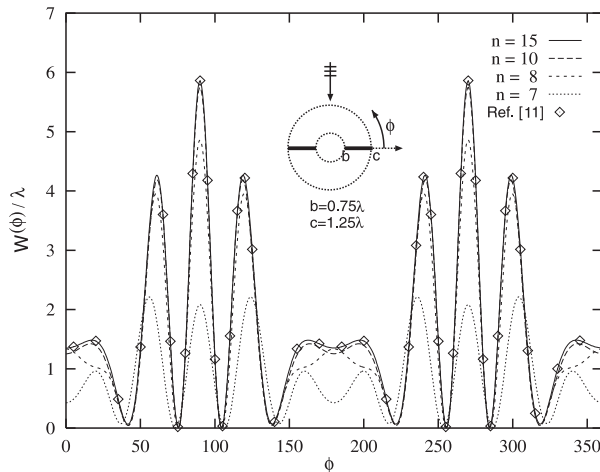
Solving the above matrices for  $A_n^\circ$  and  $D_n^\circ$ , we have

$$\begin{aligned} A_n^\circ H_n^{(2)'}(k_o c) &= (\Psi_1 - \Psi_2 \Psi_4^{-1} \Psi_3)^{-1} \Gamma - s_n H_n^{(2)}(k_o \rho_i) J_n'(k_o c) \\ D_n^\circ F_n(k_2 b) &= -\Psi_4^{-1} \Psi_3 (\Psi_1 - \Psi_2 \Psi_4^{-1} \Psi_3)^{-1} \Gamma. \end{aligned} \quad (18)$$

Once  $A_n^\circ$  and  $D_n^\circ$  are determined, the coefficient  $B_{p_m}^\circ$  and  $C_{p_m}^\circ$  can be found by using (13) and (14).

#### 4. NUMERICAL RESULTS

In order to verify that the infinite series involved in the solution is rapidly convergent, the general example is considered. The example shows the variation of the backscattering echo width for two parallel strips of  $b = 0.75\lambda_o$ ,  $c = 1.25\lambda_o$  with the number of the infinite series,  $n$ . As one can see from Fig. 4 the convergence is achieved after  $n = 15$  for a dimension of  $2.5\lambda_o$ . That is relatively a small number of terms required to achieve the convergence.



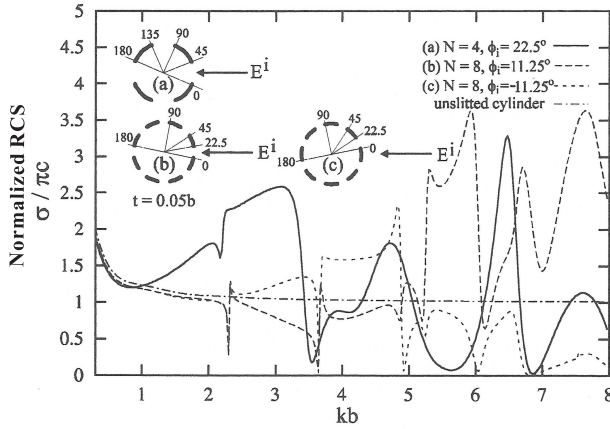
**Figure 4.** Backscattering echo width for two parallel strips of  $b = 0.75\lambda_o$ ,  $c = 1.25\lambda_o$  with the number of the infinite series number  $n$ .

Figure 5 shows the normalized backscattering (radar) cross section versus frequency ( $kb$ ) of an uncoated multi-slotted cylinder. As observed in Figs. 5(a) and (b), when the wave hits the aperture directly, the effect of resonances makes the structure strongly frequency-dependent. Therefore, RCS dependence on the angle of orientation, even if they are close to each other, will be quite different as shown in Figs. 5(b) and (c).

Figure 6 represents the radiated field versus frequency through a slot in a thick circular shell with  $\phi_1 = 60^\circ$ . The slot is filled with air and the source is an electric line current at four different positions. When the source is at the center of the shell, the resonance peaks at 2.30 and 5.42 corresponding to the  $TM_{01}$  and  $TM_{02}$  modes while the

resonance nulls at 3.83, 5.13, 6.37 and 7.01 corresponding to the  $TM_{11}$ ,  $TM_{21}$ ,  $TM_{31}$  and  $TM_{12}$  modes. Fig. 6 shows that the frequencies of resonance nulls are varied by the positions of the electric line current.

In Fig. 7, the transmission and shielding effects due to different positions of the electric current are shown by comparing contour plots



**Figure 5.** The normalized backscattering (radar) cross section versus frequency ( $kb$ ) of an uncoated multi-slotted cylinder.

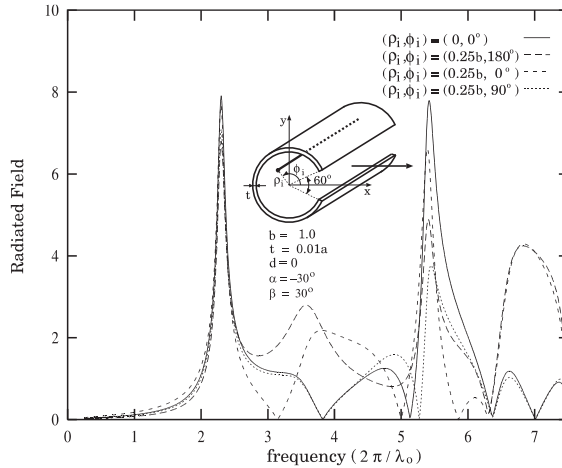


**Figure 6.** The radiated field versus frequency through a slotted circular cylinder with the electric line current at four different positions and  $\phi_1 = 60^\circ$ ,  $b = 1.0m$  and  $t = 0.01b$ .

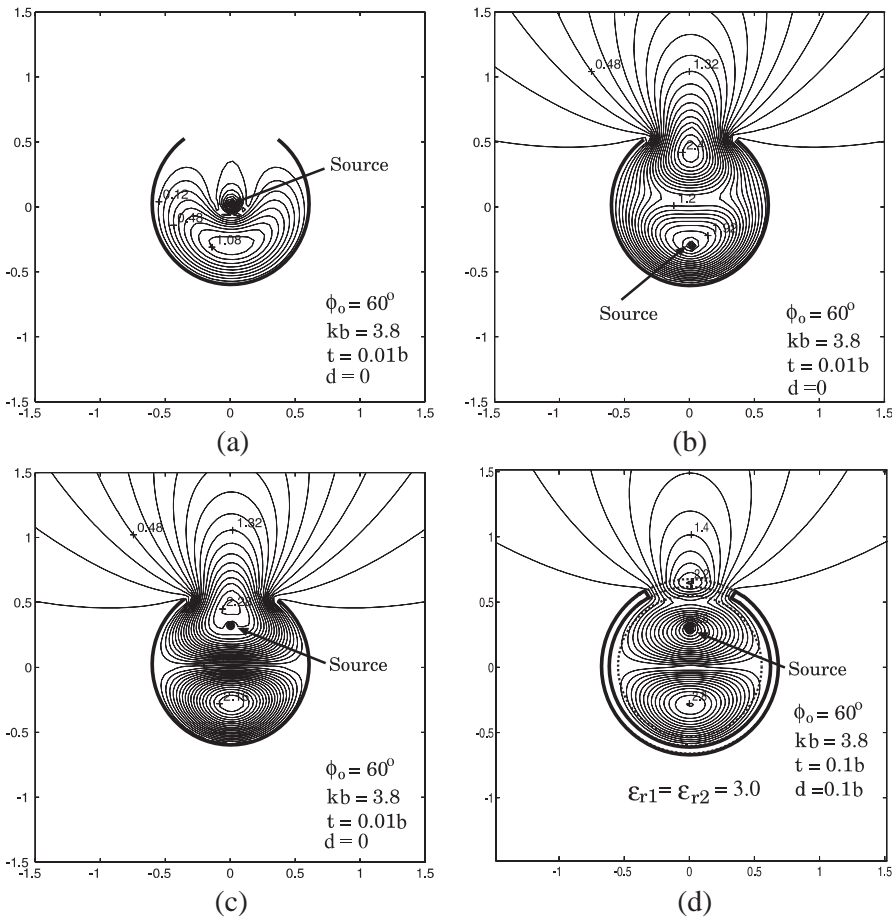
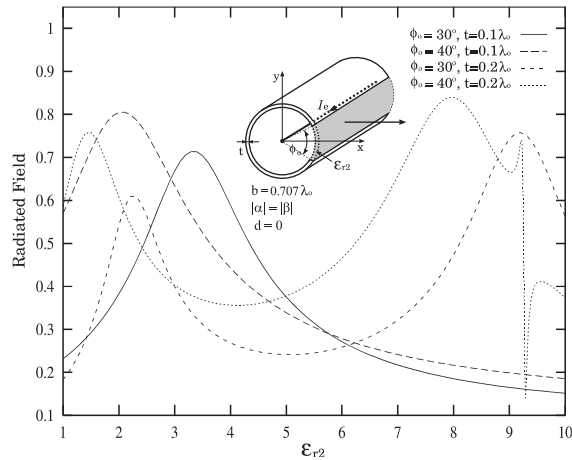


**Figure 7.** Contour plots of the electric field of a slotted circular cylinder with thickness with different positions of an electric current and  $ka = 3.8$  and  $\phi_o = 60^\circ$ .

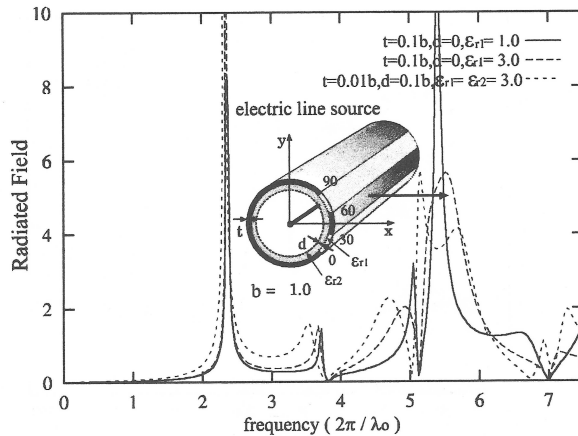
of the electric field with  $ka = 3.8$  and  $\phi_o = 60^\circ$ . In Fig. 7(a), when the source is at the center of the shell, the field is not radiated from the aperture. In contrast, the field is excited with the  $TM_{11}$  mode and radiated from the aperture in Figs. 7(b) and (c). Fig. 7(d) shows the transmission and shielding effects of covering the aperture with dielectric ( $\epsilon_{r2} = 3.0$ ,  $t = 0.1b$ ) and coating the shell with dielectric ( $\epsilon_{r1} = 3.0$ ,  $d = 0.1b$ ). It is shown that new resonance peak occurs at the thick dielectric cover.

Figure 8 shows the far field radiated through a slot in a thick

circular shell. The effect of dielectric constant on the radiated field is plotted for two different dielectric thickness and aperture width of the slot. This figure suggests that the dielectric cover over the slot causes a resonance to take place as a function of  $\epsilon_{r2}$ . For a thick dielectric, the first resonance effect is observed when  $\epsilon_{r2}$  is about 2.3 at  $\phi_1 = 30^\circ$ . When the thickness of the dielectric is reduced from  $0.2\lambda$  to  $0.1\lambda$ , the first resonance occurs at a higher value of the dielectric constant. It is



**Figure 8.** The radiated field versus  $\epsilon_{r2}$  through a dielectric-filled slotted circular cylinder with an electric line current at the center of the shell.



**Figure 9.** The radiated field versus frequency through the dielectric coated two-slotted cylinder ( $\phi_1 = \phi_2 = 30^\circ$ ) with an electric line current at the center of the shell.

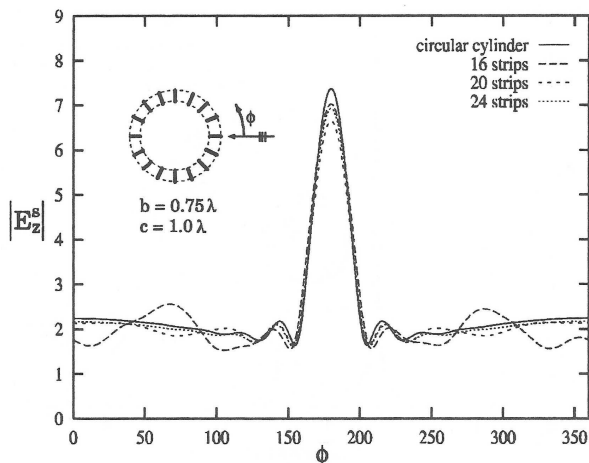


**Figure 10.** Far field patterns versus  $\phi$  for multiple-strip circle located in a radial direction with respect to the center of cylinder.

also quite surprising to see such a larger dependence on  $\varepsilon_{r_2}$  of energy radiated outside, especially for the thin dielectric case at  $0.1\lambda$ .

Figure 9 shows the radiated field versus frequency through the dielectric coated two-slotted cylinder ( $\phi_1 = \phi_2 = 30^\circ$ ) with an electric line current at the center of the shell. Fig. 10 shows the far field patterns versus  $\phi$  for multiple strips located in a radial direction with respect to the center of cylinder.

## 5. CONCLUSION

The new formulation of scattering and shielding effect of the electric line current placed inside or outside the dielectric-filled multi-slotted cylinder with thickness was presented in this paper. The radial mode matching technique was used to obtain the radiated field in series form. Radiating and coupling properties for a thick-coated multi-slotted cylinder were given for several cases.

## REFERENCES

1. Senior, T. B. A., "Electromagnetic penetration into a cylindrical cavity," *IEEE Trans. Electromagn. Compat.*, Vol. 18, 71–73, May 1976.
2. Bombardt, J. N. and L. F. Libelo, "S.E.R.A: V. surface current, tangential aperture electric field, and back-scattering cross section

- for axial slotted cylinder at normal, symmetric incidence,” *Tech. Rep. VSURFWPNCEN, NSWC/WOL/TR*, 75–39, White Oak Lab., Apr. 1975.
3. Hussein, M. I. and M. Hamid, “Scattering by a perfectly conducting cylinder with an axial infinite slot,” *Proc. Int. Symp. Recent Advances in Microwave Techniques ISRAMT91*, Aug. 1992.
  4. Hussein, M. I. and M. Hamid, “Scattering by a perfectly conducting multislot cylinder,” *Can. Journal of Physics.*, Vol. 70, 55–61, 1992.
  5. Kabalan, K. Y., A. El-Haji, and R. F. Harrington, “Characteristic modes of a slot in a conducting cylinder and their use for penetration and scattering, TM case,” *IEE Proceedings-H*, Vol. 139, No. 3, 287–291, Jun. 1992.
  6. El-Haji, A. and K. Y. Kabalan, “Scattering from and penetration into a dielectric-filled conducting cylinder with multiple apertures,” *IEEE Trans. Electromagn. Compat.*, Vol. 36, No. 3, 196–200, Aug. 1994.
  7. Colak, D., A. I. Nosich, and A. Altintas, “Radar cross-section study of cylindrical cavity-backed apertures with outer or inner material coating: The case of  $E$ -polarization,” *IEEE Trans. Antennas Propag.*, Vol. 41, No. 11, 1551–1559, Nov. 1993.
  8. Colak, D., A. I. Nosich, and A. Altintas, “Radar cross-section study of cylindrical cavity-backed apertures with outer or inner material coating: The case of  $H$ -polarization,” *IEEE Trans. Antennas Propag.*, Vol. 43, No. 5, 440–447, May 1995.
  9. Cwik, T., “Coupling into and scattering from cylindrical structures covered periodically with metallic patches,” *IEEE Trans. Antennas Propag.*, Vol. 38, Feb. 1990.
  10. Hong, W. and Z. Zhu, “Radar cross-section of dielectric-coated conducting cylinder loaded with periodic metallic strips using mixed SDM, CGM, and FFT: TE incidence,” *IEE Proceedings-H*, Vol. 140, No. 5, 373–377, Oct. 1993.
  11. Arvas, E. and T. Sarkar, “TM transmission through dielectric-filled slots in a conducting cylindrical shell of arbitrary cross section,” *IEEE Trans. Electromagn. Compat.*, Vol. 29, 150–156, May 1987.
  12. Tsalamengas, J. L., “Direct singular integral equation methods in scattering from strip-loaded dielectric cylinders,” *Journal of Electromagnetic Wave and Applications*, Vol. 10, No. 10, 1331–1358, 1996.

13. Hayashi, Y., "A singular integral equation approach to electromagnetic fields for circular boundaries with slots," *Appl. Sci. Res.*, Vol. B12, 331–359, 1965.
14. Koshparenok, V. N. and V. P. Shestopalov, "Diffraction of a plane electromagnetic wave by a circular cylinder with a longitudinal slot," *USSR Comp. Math. and Math. Phys.*, Vol. 11, 222–243, 1971.
15. Ziolkowski, R. W., W. A. Johnson, and K. F. Casey, "Application of Riemann-Hilbert problem techniques to electromagnetic coupling through apertures," *Radio Sci.*, Vol. 19, 1425–1431, Nov.–Dec. 1984.
16. Ziolkowski, R. W. and J. B. Grant, "Scattering from cavity backed apertures: The generalized dual series solution of the concentrically loaded  $E$ -pol slit cylinder problem," *IEEE Trans. Antennas Propag.*, Vol. 35, 504–528, May 1987.
17. Mautz, J. R. and R. F. Harrington, "Electromagnetic penetration into a conducting circular cylinder through a narrow slot, TE case," *Journal of Electromagnetic Wave and Applications*, Vol. 3, No. 4, 307–336, 1989.
18. Arvas, E., "Electromagnetic diffraction from a dielectric-filled slit-cylinder enclosing a cylinder of arbitrary cross section: TM case," *IEEE Trans. Electromagn. Compat.*, Vol. 31, 91–102, Feb. 1989.
19. Qin, S.-T., S.-X. Gong, R. Wang, and L.-X. Guo, "A Tdie/TDPO hybrid method for the analysis of TM transient scattering from two-dimensional combinative conducting cylinders," *Progress In Electromagnetics Research*, Vol. 102, 181–195, 2010.
20. Dumin, O. M., O. O. Dumina, and V. A. Katrich, "Evaluation of transient electromagnetic fields in radially inhomogeneous nonstationary medium," *Progress In Electromagnetics Research*, Vol. 103, 403–418, 2010.
21. Bucinkas, J., L. Nickelson, and V. Sugurovas, "Microwave scattering and absorption by a multilayered lossy metamaterial — Glass cylinder," *Progress In Electromagnetics Research*, Vol. 105, 103–118, 2010.
22. Bucinkas, J., L. Nickelson, and V. Sugurovas, "Microwave diffraction characteristic analysis of 2D multilayered uniaxial anisotropic cylinder," *Progress In Electromagnetics Research*, Vol. 109, 175–190, 2010.
23. Sirenko, K., V. Pazynin, Y. K. Sirenko, and H. Bagci, "An FFT-accelerated FDTD scheme with exact absorbing conditions for characterizing axially symmetric resonant structures," *Progress In Electromagnetics Research*, Vol. 111, 331–364, 2011.

24. Bui, V. P., X. C. Wei, E. P. Li, and W. J. Zhao, "An efficient hybrid technique for analysis of the electromagnetic field distribution inside a closed environment," *Progress In Electromagnetics Research*, Vol. 114, 301–315, 2011.
25. Ashraf, M. A. and A. A. Rizvi, "Electromagnetic scattering from a random cylinder by moments method," *Journal of Electromagnetic Wave and Applications*, Vol. 25, No. 4, 467–480, 2011.
26. Zubair, M., M. J. Mughal, and Q. A. Naqvi, "An exact solution of the cylindrical wave equation for electromagnetic field in fractional dimensional space," *Progress In Electromagnetics Research*, Vol. 114, 443–455, 2011.
27. Tan, W., W. Hong, Y. Wang, and Y. Wu, "A novel spherical-wave three-dimensional imaging algorithm for microwave cylindrical scanning geometries," *Progress In Electromagnetics Research*, Vol. 111, 43–70, 2011.
28. Jandieri, V., K. Yasumoto, and Y.-K. Cho, "Rigorous analysis of electromagnetic scattering by cylindrical EBG structures," *Progress In Electromagnetics Research*, Vol. 121, 317–342, 2011.
29. Park, J. E., K. Y. Kim, and J.-W. Song, "Resonant power transmission trough coupled subwavelength ridged circular apertures," *Journal of Electromagnetic Wave and Applications*, Vol. 26, No. 4, 423–435, 2012.